

SUPPORTING INFORMATION for:

**Broadband achromatic anomalous mirror in
near-IR and visible frequency range**

Andrei Nemilentsau* and Tony Low*

*Department of Electrical & Computer Engineering, University of Minnesota, Minneapolis,
MN 55455, USA*

E-mail: anemilen@umn.edu; tlow@umn.edu

Derivation of gap plasmon dispersion

In order to design the achromatic anomalous mirror, we use the metal-insulator-metal (MIM) resonators as building blocks. The wave impinging on this resonator excites a gap plasmon. An additional phase acquired by the plasmon, propagating back and forth inside the resonator before re-radiating its energy back to space, is

$$\Phi \approx 2h\text{Re}\beta, \quad (1)$$

where h is the resonator length, where β is the plasmon wavenumber

Dispersion relation for gap plasmons in the MIM structures is well-known and is given by¹

$$\tanh \frac{\gamma_d a}{2} = -\frac{\gamma_m \varepsilon_d}{\gamma_d \varepsilon_m}, \quad (2)$$

where ε_d and ε_m are relative permittivities of dielectric and metal, respectively, while $\gamma_i = \sqrt{\beta^2 - k_i^2}$, and $k_i^2 = k_0^2 \varepsilon_i$. In what follows, we assume that in the frequency range under consideration, the permittivity of metal can be approximated by the Drude model

$$\varepsilon_m = \varepsilon_\infty - \frac{\omega_p^2}{\omega^2 + i\gamma\omega}, \quad (3)$$

where ε_∞ is the metal permittivity at high frequencies, ω_p is a plasma frequency, and γ is a relaxation frequency.

Let us assume that $\gamma_d a \ll 1$. In this case the dispersion relation (2) can be rewritten

$$\frac{\gamma_d a}{2} = -\frac{\gamma_m \varepsilon_d}{\gamma_d \varepsilon_m} \quad (4)$$

or

$$\begin{aligned}
\gamma_d^2 &= -\frac{2\gamma_m \varepsilon_d}{a \varepsilon_m} \quad \Rightarrow \quad \gamma_d^4 = \frac{4\gamma_m^2 \varepsilon_d^2}{a^2 \varepsilon_m^2}, \\
(\beta^2 - k_d^2)^2 &= (\beta^2 - k_m^2) \frac{4\varepsilon_d^2}{a^2 \varepsilon_m^2}, \\
\beta^4 - 2\beta^2 k_d^2 + k_d^4 &= (\beta^2 - k_m^2) \frac{4\varepsilon_d^2}{a^2 \varepsilon_m^2}, \\
\beta^4 - 2\beta^2 \left(k_d^2 + \frac{2\varepsilon_d^2}{a^2 \varepsilon_m^2} \right) + k_d^4 + k_m^2 \frac{4\varepsilon_d^2}{a^2 \varepsilon_m^2} &= 0, \\
\beta^4 - 2\beta^2 \varepsilon_d \left(k_0^2 + \frac{2\varepsilon_d}{a^2 \varepsilon_m^2} \right) + k_0^2 \varepsilon_d^2 \left(k_0^2 + \frac{4}{a^2 \varepsilon_m} \right) &= 0.
\end{aligned}$$

In the frequency range where $\gamma \ll \omega_p$ and $\omega \ll \omega_p$, the Drude dielectric function can be approximated as

$$\varepsilon_m \approx -\frac{\omega_p^2}{\omega^2} = -\frac{\omega_p^2}{k_0^2 c^2} \quad (5)$$

Then the dispersion equation can be further simplified as

$$\beta^4 - 2\beta^2 k_0^2 \varepsilon_d \left(1 - \frac{2\varepsilon_d k_0^2 c^4}{a^2 \omega_p^4} \right) + k_0^4 \varepsilon_d^2 \left(1 - \frac{4c^2}{a^2 \omega_p^2} \right) = 0.$$

For the metasurface design in the paper we used silver as the metal. The parameters of Drude model for the silver take the values² $\varepsilon_\infty = 1$, $\omega_p = 1.37 \times 10^{16} \text{ s}^{-1}$, $\gamma = 2.73 \times 10^{13} \text{ s}^{-1}$. Let us estimate terms in the brackets in the above equation, i.e.

$$\begin{aligned}
\frac{4c^2}{a^2 \omega_p^2} &\approx 0.19 \\
\frac{2\varepsilon_d k_0^2 c^4}{a^2 \omega_p^4} &= \frac{\varepsilon_d}{2} \frac{4c^2}{a^2 \omega_p^2} \frac{\omega^2}{\omega_p^2} \approx 0.95 \varepsilon_d \frac{\omega^2}{\omega_p^2} \ll 1,
\end{aligned}$$

where $a = 100 \text{ nm}$ (the largest width we used in simulations), and we also took into account that we are working in the frequency range where $\omega/\omega_p \ll 1$. In this case we can simplify

dispersion equation even further:

$$\beta^4 - 2\beta^2 k_0^2 \varepsilon_d + k_0^4 \varepsilon_d^2 \left(1 - \frac{4c^2}{a^2 \omega_p^2}\right) = 0.$$

The solution of this quadratic equation is

$$\beta = k_0 \sqrt{\varepsilon_d \left(1 + \frac{2c}{a\omega_p}\right)} \quad (6)$$

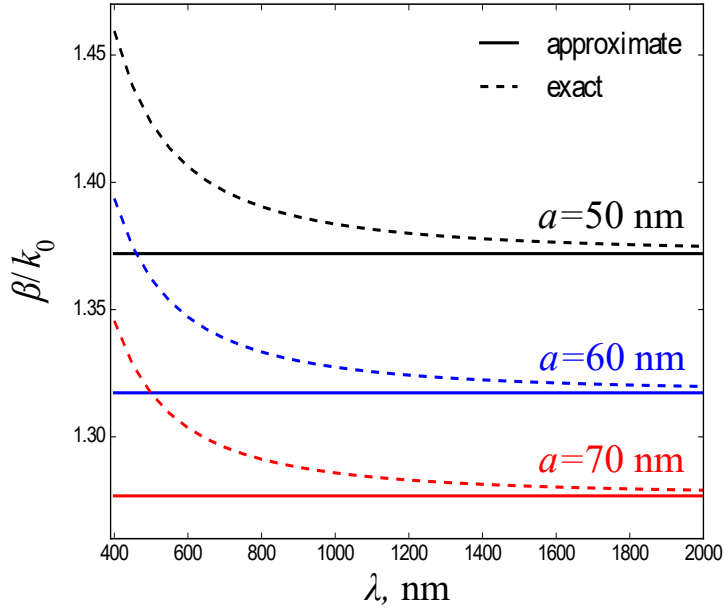


Figure 1: Normalized gap plasmon wavenumber β/k_0 for different gap widths, a , as a function of radiation wavelength for the silver-air-silver resonator.

By substituting Eq. (6) into Eq. (1) we obtain

$$\Phi(\omega, x) = k_0 2h(x) \sqrt{\varepsilon_d(x) \left(1 + \frac{2c}{a(x)\omega_p}\right)}. \quad (7)$$

Comparison between gap plasmon propagation constants, β , calculated using exact equation (2) and approximate equation (6), is presented in Fig. 1 for the case of the silver-air-silver resonator and for different gap widths, a . One can see that Eq. (6) is a good approximation

for the gap plasmon wavenumber over a broad frequency range from near-IR up to visible. However, the approximation becomes less reliable at higher frequencies beyond $\lambda = 400$ nm ($\omega = 0.47 \times 10^{16}$ rad/s) as the radiation frequency becomes comparable to the plasma frequency ω_p in silver. Thus the approximate expression for the accumulated phase, Eq. (7), is valid in the near-IR and visible frequency ranges.

Total electric field for the case presented in Figs. 2a,b in the main text

Figure 2 presents distribution of the intensity of total electric field in the system for the case presented in Figs. 2a,b of the main text.

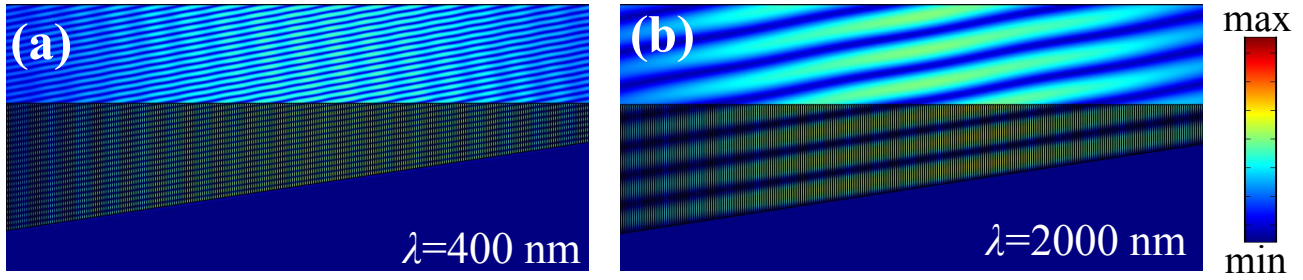


Figure 2: Spatial distribution of intensity of total electric field, $|\mathbf{E}_{tot}|$ for the cases presented in Figs. 2a,b of the main text.

Sensitivity of device parameters to imperfections in device geometry

The results presented so far were obtained assuming that length, h_i , of each resonator is equal exactly to the desired length defined by Eq. (10) in the manuscript. However, resonators lengths naturally fluctuates during fabrication. In order to study the effect of these fluctuations on the mirror performance we simulated the metasurface assuming that lengths of each resonator is equal to $h_i + \delta_i(\mu)$, where h_i is the desired ideal length defined by Eq. (10), while $\delta_i(\mu)$ is sampled

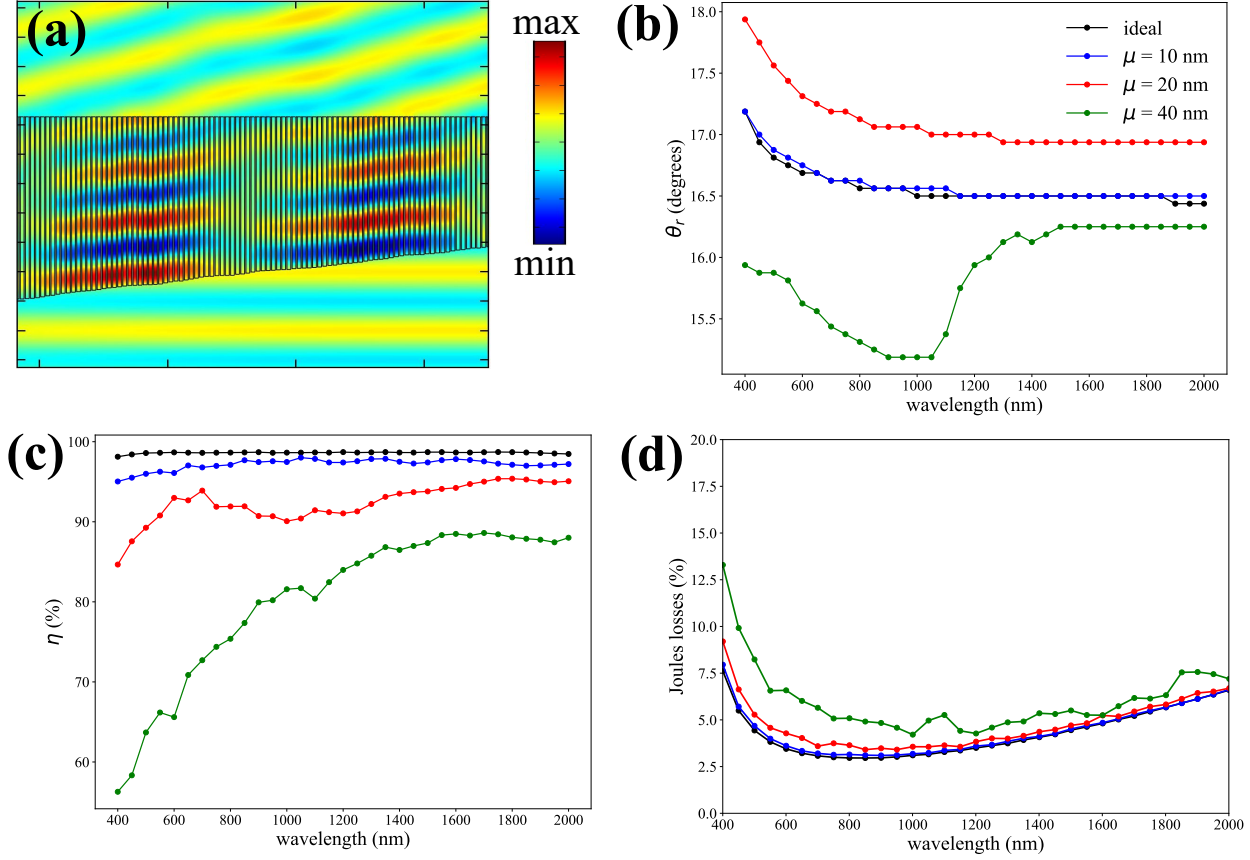


Figure 3: (a) Geometry of the metasurface accounting for fabrication introduced fluctuations in resonators lengths, $h_i + \delta_i(\mu)$, where h_i is an ideal length of resonator defined by Eq. (10) in the manuscript, while $\delta_i(\mu)$ is sampled randomly from uniform distribution on interval $[-\mu, \mu]$. In this case $\mu = 20$ nm. (b, c, d) Steering angle, θ_r , radiation efficiency, η , Joule losses for different scales of fluctuations, μ . The mirror consists of $N = 450$ resonators of width $d = 80$ nm each. Gap width $a = 60$ nm.

randomly from uniform distribution on interval $[-\mu, \mu]$. Simulation results are presented in Fig. 3. As one can see, device performance is not significantly affected by the resonators lengths fluctuations on $2\mu = 20$ nm scale. The device still demonstrates good performance for fluctuations on 50 nm scale, but performance deteriorates fast when the fluctuations become as large as 100 nm.

Large steering angles

In the manuscript we demonstrated that anomalous mirror based on MIM resonators has excellent performance characteristics up to a steering angle of 40° . However, as one can see in Fig. 4 with the increase of steering angle above 40° performance characteristics deteriorate fast, especially in visible range.

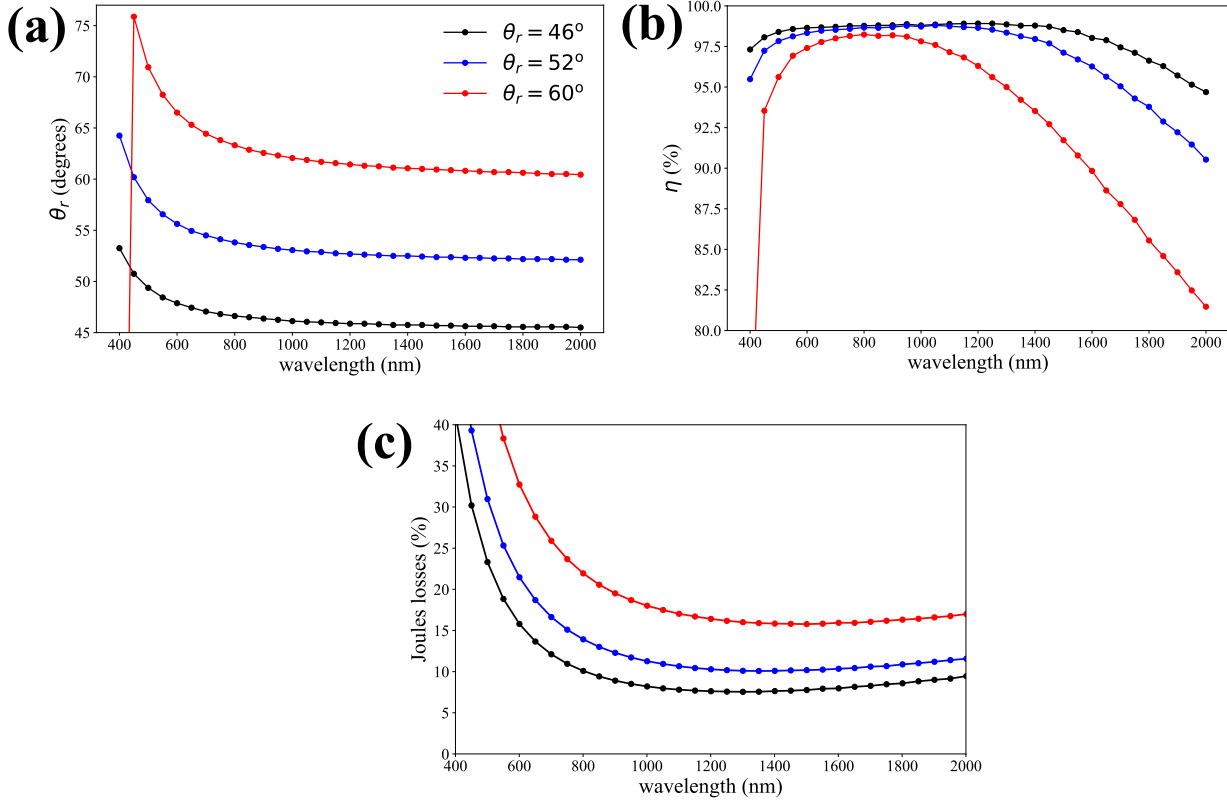


Figure 4: Steering angle, θ_r , radiation efficiency, η , and Joules losses for an anomalous mirror steering normally incident beam to large angles indicated in panel (a). The mirror consists of $N = 450$ resonators of width $d = 80$ nm each. Gap width $a = 60$ nm.

References

- (1) Stefan Alexander Maier. *Plasmonics: fundamentals and applications*. Springer Science & Business Media, 2007.

- (2) M. A. Ordal, Robert J. Bell, R. W. Alexander, L. L. Long, and M. R. Query. Optical properties of fourteen metals in the infrared and far infrared: Al, co, cu, au, fe, pb, mo, ni, pd, pt, ag, ti, v, and w. *Appl. Opt.*, 24(24):4493–4499, Dec 1985.